Space situational awareness of large numbers of payloads from a single deployment

Alan M. Segerman, Jeff M. Byers, John T. Emmert, and Andrew C. Nicholas
Naval Research Laboratory

ABSTRACT

The nearly simultaneous deployment of a large number of payloads from a single vehicle presents a new challenge for space object catalog maintenance and space situational awareness (SSA). Following two cubesat deployments in November, 2013, five weeks were required to catalog the resulting 64 orbits. The Kicksat mission of May, 2014, if it had proved successful, would have presented an even greater SSA challenge, with its deployment of 128 chip-sized picosats. Although all of these deployments were in short-lived orbits, future deployments will inevitably occur at higher altitudes, with a longer term threat of collision with active spacecraft.

With such deployments, individual scientific payload operators require rapid precise knowledge of their satellites' locations. Following the first November launch, the cataloging did not initially associate a payload with each orbit, leaving this to the satellite operators. For short duration missions, the time required to identify an experiment's specific orbit may easily be a large fraction of the spacecraft's lifetime. For a Kicksat-type deployment, present tracking cannot collect enough taggable observations to catalog each small object. The current approach is to treat the chip cloud as a single catalog object. However, the cloud dissipates into multiple subclouds and, ultimately, tiny groups of untrackable chips.

One response to these challenges may be to mandate installation of a transponder on each spacecraft. Directional transponder transmission detections could be used as angle observations for orbit cataloging. Of course, such an approach would only be employable with cooperative spacecraft. In other cases, a probabilistic association approach may be useful, with the goal being to establish the probability of any element being at a given point in space. This would permit more reliable assessment of the probability of collision of active spacecraft with any cloud element.

This paper surveys the cataloging challenges presented by large scale deployments of small spacecraft, examining current methods. Potential new approaches are discussed, including simulations to evaluate their utility.

1. INTRODUCTION

The advent of large numbers of satellite deployments from a single space launch presents a new challenge to the task of space object catalog maintenance. While launches formerly led to a small number of active payloads to be cataloged, now a single launch can result in dozens of objects, usually small cubesats. Additionally, the deployments can take place nearly simultaneously, further complicating the cataloging effort. This situation presents a new paradigm that must be addressed in order to maintain adequate space situational awareness (SSA).

Such deployments are becoming common, with several recent large-scale deployments of cubesats both from carrier launch vehicles and the International Space Station. From a cataloging standpoint, in some ways these deployments are similar to orbital debris events, only planned. Indeed, to a large extent, current cataloging already satisfies operational SSA needs.

However, in the crowded space environment presented by such deployments, it remains difficult to identify the specific payloads associated with each catalog entry. As such, the orbit cataloging is insufficient to satisfy the requirements of the cubesat community. Cubesats are often orbited to test or demonstrate novel techniques or operating modes; therefore, the individual satellite operators require rapid and precise knowledge of the locations of their satellites. For short duration missions, a lengthy identification period may easily be a large fraction of the spacecraft's orbital or operational lifetime. Therefore, in order for cubesats to fulfill their potential, it is necessary to improve the speed of their identification subsequent to their deployment.

An even greater challenge is posed by the near-simultaneous deployment of many picosats, or "satellites on a chip." While cubesats may be difficult to catalog, the cataloging of these chipsats is nearly impossible, as present tracking

capabilities do not permit collecting sufficient observations of each small object to form catalogable orbits. From an SSA standpoint, it is fortunate that currently planned chipsat deployments are planned at low altitudes, with the high area-to-mass ratio objects having relatively short orbital lifetimes. However, future deployments are likely to occur at higher altitudes, with the attendant longer term threat of collision with active spacecraft.

Currently, SSA maintenance is likely to be attempted on such a set of chips by endeavouring to catalog the entire chip cloud as a single space object. Observations of any of the cloud elements would then be correlated with that single object. While this may provide a gross estimate of the cloud's position, the inability to locate the individual chips means that it is not possible to reliably predict collisions of chips with other spacecraft — a key SSA application for catalog orbits. One potential alternative would be the use of a probabilistic association approach, in which the goal is not to catalog each element of the cloud but rather to establish the probability of any element being at some given point in space. In this manner, it would be possible to more reliably assess the probability of collision of any cloud element with an active spacecraft, regardless of exactly which element it may be. Methods of debris cloud collision assessment and analysis, such as those already being developed in the 1990s [1, 2] could then be employed.

2. CUBESAT DEPLOYMENT AND CATALOGING

The nearly simultaneous deployment of large numbers of cubesat spacecraft, sized at multiples of 10 cm on a side, has moved from the realm of the hypothetical to the realm of the possible, and now to the realm of the ordinary. As seen in the blue bars of Fig. 1, multi-satellite payload launches with at least three payloads have increased in frequency since 2004, but most significant are the three large-scale deployments in 2013 and 2014. Within two days in November, 2013, two missions deployed 29 and 32 cubesats, from Wallops Island, Virginia, and Dombarovsky Air Base in Russia, respectively; in June, 2014, 38 cubesats were deployed from another Dombarovsky mission [3]. Additionally, the number and frequency of deployments from the International Space Station have also increased. Over 17 days in February, 2014, 33 cubesats were deployed in batches from the International Space Station (ISS), with the final five being deployed together. Prior to that time, only 11 payloads had been deployed from the ISS, four of those in November, 2013. (Deployments from the ISS are shown in the red bars of Fig. 1, with multi-day series of deployments grouped together.)

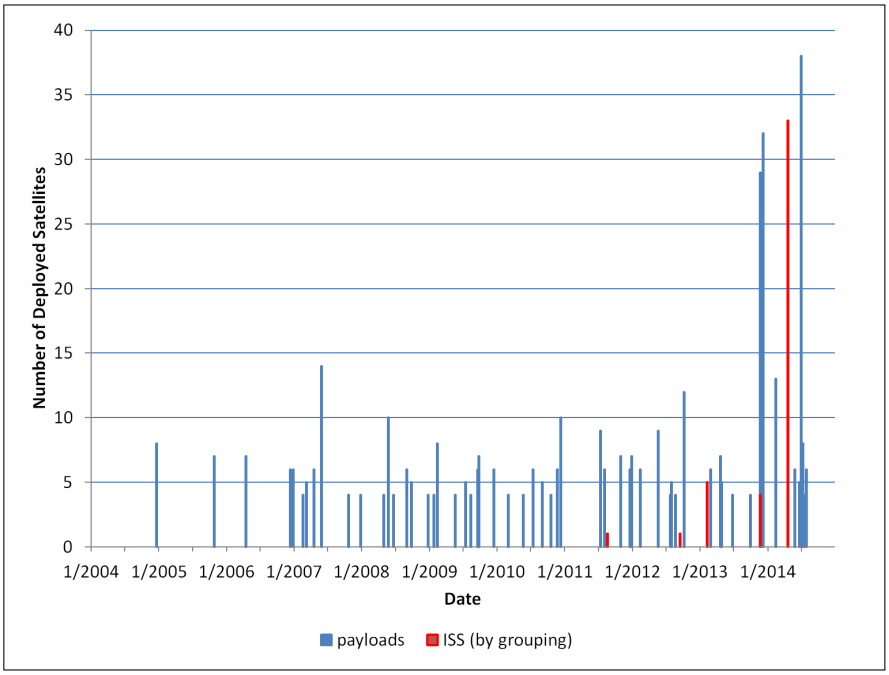

Fig. 1. Multiple Payloads (at least 3) in a Single Launch, 2004–2014 (red = ISS deployments by series) [3]

From a cataloging perspective, the pace at which the orbits are cataloged has seemed to improve, although the sample set of large-scale deployments performed remains small. Fig. 2 shows the evolution of this pace. The figure shows

that five weeks were required to catalog the orbits resulting from the Wallops launch. The orbits from the first Dombarovsky launch took 13 days to catalog (with perhaps a higher level of Space Surveillance Network (SSN) sensor tasking than for the Wallops launch), and cataloging the orbits from the 2014 Dombarovsky launch took only four days. Not surprisingly, orbits of objects deployed from the ISS have consistently been cataloged at a more rapid pace; even here, the rate has increased, with the most recent deployment taking less time on average.

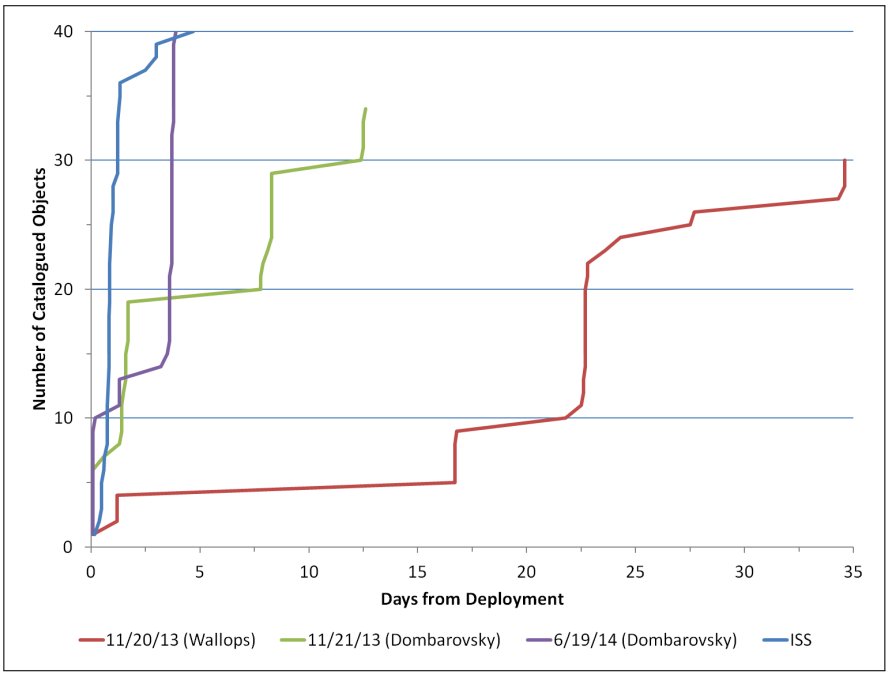

Fig. 2. Pace of Multiple Payload Deployment Cataloging (ISS deployments grouped together) [3–5]

The cataloging and tracking challenges are made more acute by the small size of the cubesats and the decommissioning of the former Air Force Space Surveillance System (AFSSS). The AFSSS, or Space Fence, operated in an uncued manner, permitting it to collect observations of any objects that passed through the plane of its radar energy. Even so, many cubesats are too small to have been reliably detected by the AFSSS, which operated in the VHF band. The new S-band Space Fence will have improved tracking capabilities, but will not be operational until at least 2018, and will still have limitations on its ability to track the small cubesats.

Recognizing this challenge, the Joint Space Operations Center (JSpOC), the entity with responsibility for adding orbits to and maintaining the space object catalog, has begun soliciting information from the cubesat community to assist in its cataloging efforts, particularly its efforts to correctly identify the orbiting cubesats. In the case of the June, 2014, deployment, JSpOC made such a solicitation to the owner-operators of the cubesats as part of its JSpOC SSA Sharing initiative. In particular, JSpOC announced that it would initially rely on SSN data, “but with your inputs and feedback we believe that we can expedite identification and avoid incorrect naming [6].”

As noted above, cubesat operators generally require rapid and precise knowledge of the locations of their satellites. In the case of the November launch from Wallops, even once the 30 orbits were all cataloged, the cataloging did not definitively identify which payload was associated with each orbit, leaving this exercise to the satellite operators.

One case illustrates some of the difficulties of matching the cataloged orbits with the individual spacecraft. As part of the February, 2014, series of cubesat deployments from the ISS, SkyCube was deployed nearly simultaneously with four other cubesats, and within only several weeks of 28 other cubesat deployments from the ISS. The SkyCube investigators anticipated identifying their spacecraft within days. However, despite the fact that all of the deployments were carefully monitored, noting the precise release times and sequence, and that the orbits were all cataloged within 32 hours of the respective deployments, it took weeks to conclusively identify SkyCube within the crowded cubesat environment.

This delay was caused by a number of factors, including uncertainty over which satellite the SkyCube operators were to target with their interrogation signal, as it quickly became clear that JSpOC's tentative pairing of the spacecraft identities with the orbits was incorrect. The SkyCube team did engage in cooperative efforts with developers of the other deployed cubesats and took advantage of the efforts of the amateur radio community in slowly determining which orbiting spacecraft was SkyCube [7]. The common problem is that, in the absence of conclusive orbit tagging, payload operators do not know which spacecraft to attempt to contact or, in the case of automatically beaconing cubesats, when to listen for the signal. The cubesat investigators do not necessarily have the directional sensitivity to distinguish among the catalog objects until sufficient separation has occurred but, even then, trial and error has been the standard approach to forming a definitive identification.

With the lessons learned from these large-scale deployments, the cubesat community has already begun developing techniques for speeding the satellites' identification in a crowded environment. One option under consideration is to have the cubesats continually beacon an identifiable signal on a specified frequency, perhaps using radio-frequency identification (RFID) chips. During the time while a milliwatt transponder would operate, a ground receiving station could use the signal's directional orientation to provide a satellite observation that is tagged to the specific spacecraft. This data would be useful for both object identification and, in conjunction with existing observational data, for improvement of orbit tracking [8, 9].

A second approach being investigated involves the use of GPS. While some cubesats have contained GPS receivers, the location information has not typically been part of their beacon signals. GPS position and time information could be transmitted by an identifiable beacon from a cubesat on a predefined broadcast frequency at a predetermined rate. This data could then be collected by ground stations and processed as part of the orbit determination. However, the data quantity would be limited by the duration of the beacon's time within range of the ground stations. A more robust version of this method would involve transmitting the GPS data via satellite communications, using an orbiting communications constellation such as Iridium, Globalstar, or TDRSS. This would permit reception of the signal over the entire orbit, enabling much faster orbit determination [8, 10]. During April-May, 2014, the TSAT cubesat demonstrated the use of Globalstar to transmit scientific data [11]; GPS location data could be similarly transmitted.

At present, the use of onboard GPS for cubesat identification poses several challenges. For example, commercially available receivers are optimized for terrestrial operation — their software algorithms are not tuned to accommodate the large Doppler variations in the received signal frequencies that are experienced in orbit or the rapid changes in satellite visibility that accompany the orbital motion. Also, orbital altitude and velocity exceed limits imposed by International Traffic on Arms Regulations (ITAR) requirements, originally instituted to preclude the use of GPS receivers on ballistic missiles. And, commercial GPS receivers are not designed for the harsh space environment. Cubesat developers are investigating both hardware and software solutions to these challenges [12].

3. CHIPSAT CLOUD DEPLOYMENT AND CATALOGING

One of the six satellites deployed as part of the April 18, 2014, Falcon 9 launch to the ISS was Kicksat. Kicksat's planned mission involved a near-simultaneous deployment of 128 chip-sized picosats or "sprites." While a technical problem with Kicksat's controller prevented the chip deployment from occurring during the spacecraft's orbital lifetime, the planned mission illustrates another SSA challenge presented by large-scale deployments.

As mentioned above, tracking sensors do not currently possess the ability to track each sprite in a cloud in order to catalog each individual sprite's orbit. Instead, the cloud itself would be treated as a single catalog object, with any individual sprite observations correlated to it. However, this does not permit adequate estimation of the collision risks posed by any individual chip to an active spacecraft. It may be possible to obtain tracking assistance from the sprite owner-operator (in the case of Kicksat, a group at Cornell University). Of course, such assistance would only be available from a cooperative owner-operator and, even then, there are substantial limitations to the position resolution that could be obtained for the individual sprites. In the more general case, in which spacecraft within a large deployment may be uncooperative or even launched with nefarious intent, it would be preferable to employ a probabilistic association approach, in which the probability could be assessed of any cloud element being at a given location. In this manner, it would be possible to more reliably assess the probability of collision of any cloud element with an active spacecraft, regardless of exactly which element it may be.

One such probabilistic approach could take advantage of the batch least squares orbit determination already implemented within the current operational cataloging paradigm. Consider the batch least squares differential correction of an epoch element set represented by $\mathbf{e}$. The element correction at each iteration of the process is the solution of the normal equations, given by

$$\Delta\mathbf{e} = \left[\sum_i \left(A_i{}^{\mathrm{T}} W_i A_i\right)\right]^{-1} \sum_i \left(A_i{}^{\mathrm{T}} W_i \Delta\mathbf{b}_i\right), \tag{1}$$

where $\Delta\mathbf{b}_i$ is the vector of component residuals from an individual satellite observation, A_i is the Jacobian relating observation space to epoch element space, and W_i is the diagonal weight matrix containing the inverse variances of the observation. Note that the matrix inverse appearing in Eq. (1) is assumed to exist.

For purposes of notation, let

$$A^{\mathrm{T}} W \Delta\mathbf{b} = \sum_i \left(A_i^{\mathrm{T}} W_i \Delta\mathbf{b}_i\right)$$

and

$$A^{\mathrm{T}} W A = \sum_i \left(A_i^{\mathrm{T}} W_i A_i\right). \tag{2}$$

Then, Eq. (1) may be written formally as

$$\Delta\mathbf{e} = \left(A^{\mathrm{T}} W A\right)^{-1} \left(A^{\mathrm{T}} W \Delta\mathbf{b}\right), \tag{3}$$

providing the solution to the associated normal equation

$$A^{\mathrm{T}} W A \Delta\mathbf{e} = A^{\mathrm{T}} W \Delta\mathbf{b}.$$

The covariance provided by the orbit determination process is the inverse of the matrix given in Eq. (2). Denoting this epoch covariance matrix as C,

$$C = \left(A^{\mathrm{T}} W A\right)^{-1}.$$

The diagonal elements of C represent the variances of the corresponding variables; the off diagonal elements represent the relevant covariances, which indicate the variables' relative interdependence. Using standard eigenvalue problem techniques, the covariance matrix may be diagonalized to give what may be called the principal covariances and principal covariance axes. This description of the error distribution is analogous to the eigenvalue problem analysis of an inertia matrix describing a system's mass distribution, in which the eigenvalues and eigenvectors represent the principal inertia moments and axes. Here, the eigenvalues and eigenvectors provide the size and orientation of an equiprobability error ellipsoid in the specified element space. As with the inertia matrix, because the covariance matrix is positive definite, these principal covariances are guaranteed to be positive as well.

In operational catalog maintenance, the weight matrices W_i of Eq. (1) are populated using the inverses of static calibration variances developed for each sensor. For the case of a sprite cloud, say that a sensor cannot form observations for each sprite but that it can be tasked to identify the cloud as a trackable entity. Additionally, in an oversimplified representation of the sensor tracking, say that the sensor can, through its internal filtering mechanism, discern the cloud's centroid and distribution in observation space, with the distribution being represented as statistical variances. Then, within the batch least squares process, the centroid could be treated as an observation of the cloud as a single entity and the variances used as the observation weights. This is similar to using the mean and variance statistics from a Monte Carlo sampling to represent a data distribution. The epoch state resulting from the weighted batch least squares differential correction then serves as an estimate of the state of the cloud's centroid, while the covariance C provides an estimate of the statistical distribution of the cloud's elements at epoch.

In the context of a batch least squares differential correction, Barker, Casali, and Walker demonstrated that observations within a single track are highly autocorrelated; treating them as though they were independent, results in a highly overoptimistic covariance [13]. Rather, covariance realism is improved by averaging the contributions from a track's observations — that is, dividing the entries of an observation's weight matrix by the number of observations

in the track. Similarly, the mean/variance statistics for the sprite cloud observations are autocorrelated, as they represent the evolution of the cloud's constituents under orbital dynamics. Therefore, in performing the differential correction of the cloud orbit, the observations are also deweighted, here by the total number of centroid observations.

4. CHIPSAT CLOUD CATALOGING SIMULATION

A simulation was used to demonstrate the utility of the probabilistic approach described in Section 3. Consider the deployment of 128 sprites from a Kicksat-class cubesat (10 cm $\times$ 10 cm $\times$ 30 cm). As with Kicksat, the sprites were presumed to be initially stacked in four stacks of 32 sprites each. The sprites are each 5 g in mass, 3.5 cm on a side, and 3 mm thick. At deployment, the cubesat was assumed to be spinning about its long axis, imparting a ΔV of 7.5 cm/s to the chips, in a different direction for each chip stack. This is consistent with the planned Kicksat sprite deployment shown in Fig. 3 [14].

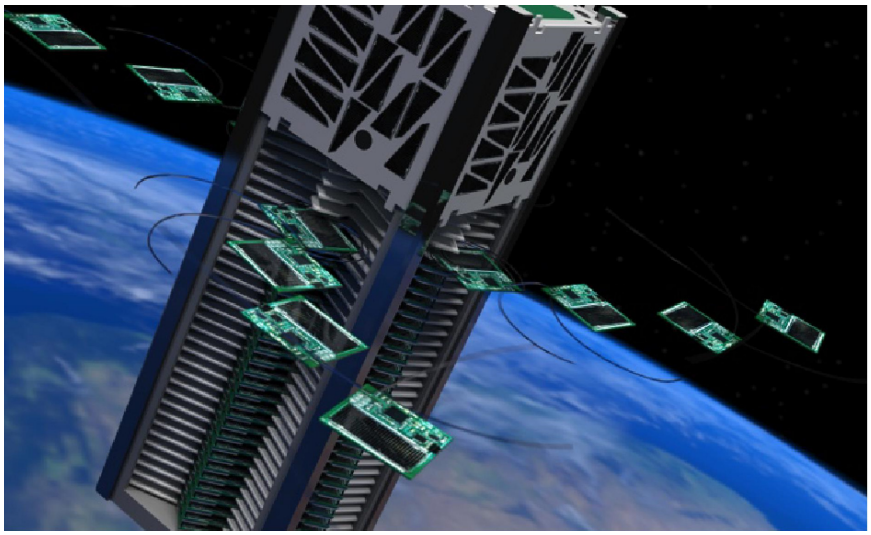

Fig. 3. Kicksat Sprite Deployment [14]

For the purpose of this simulation, the deployment was assumed to take place when the cubesat crossed the equator and, for convenience, when the ascending node of the orbit was at zero longitude, and at approximately noon UTC. To achieve maximum chip dispersion, the long axis of the cubesat was taken to be aligned with the orbit's radial direction, and the four deployment directions to be in and normal to the orbit plane. (This differs somewhat from the preferred Kicksat deployment, where the chip faces were to be sun-facing in order to obtain maximum solar energy on the chips' solar cells.) The cubesat orbit parameters were derived from the actual Kicksat orbit and are given in Table 1.

Table 1. Simulated Kicksat Orbit Parameters

semimajor axis	6693.515 km
eccentricity	0.00238
inclination	51.653 deg

For a deployment from this configuration, a two-day truth ephemeris was generated for each chip. In each chip's propagation, a ballistic coefficient of 0.5 m^2/kg was used. This roughly corresponds to the flat side surface area, with a drag coefficient of 2.2, as suggested in [15] and [16]. The ephemerides were formed at 15 second steps, using the propagator that is part of the SPeCIAL-K catalog maintenance software package, developed at the Naval Research Laboratory and used operationally at JSpOC's Distributed Space Command and Control detachment in Dahlgren, Virginia (DSC2-Dahlgren). SPeCIAL-K uses an 8^{th}-order Gauss-Jackson special perturbations integrator and permits a variety of force models and control parameters for orbit determination and propagation [17]. This propagation was performed using 36×36 WGS-84 geopotential, lunisolar gravitational perturbations, and the Jacchia-70 drag model.

From the truth ephemerides, noise-free azimuth/elevation/range observations were constructed for a radar site located at approximately 30.57 deg. north latitude, 86.22 deg. west longitude (the location of the space surveillance network radar at Eglin AFB in Florida). Assuming that, given appropriate tasking, Eglin could estimate the chip cloud distribution, the cloud's mean and standard deviation was determined in observation space for each time step for which the cloud was visible from Eglin. One day of these data was then treated as sensor observations in a batch least squares differential correction of the cloud orbit, with the carrier vehicle's orbit as the initial estimate for the cloud state. The cloud means were used as the observations and the inverses of the squared standard deviations were used as observation weights, in place of the usual static weights. The orbit determination was performed using a variant of the orbit determination routine within SPeCIAL-K, and the state epoch was placed at the time of the last observation within the one day span.

The SPeCIAL-K batch least squares differential correction is performed using equinoctial elements, nonsingular for circular and equatorial orbits [18]. The set used, forming a six-dimensional space, is defined as:

$f =$ cosine of perigee longitude, scaled by eccentricity
$g =$ sine of perigee longitude, scaled by eccentricity
$L =$ mean longitude
$n =$ mean motion
$\chi =$ sine of ascending nodal right ascension, scaled by subsidiary parameter ζ
$\psi =$ cosine of ascending nodal right ascension, scaled by subsidiary parameter ζ

where ζ is a function of the inclination, given by $\zeta = \sin I/(1+\cos I)$.

The utility of the element covariance resulting from the differential correction, as a representation of the sprite cloud distribution, was then evaluated. This covariance was propagated for one day subsequent to the epoch of the differentially corrected state, to the times of the second day of the truth ephemerides, and transformed to radial/tranverse/orbit normal (*uvw*) space. The covariance propagation and transformation were performed as follows.

Let the vector $\mathbf{e}(t)$ refer to the epoch equinoctial element vector as propagated from epoch time t_0 to time t, and let Φ denote the state transition matrix,

$$\Phi(t,t_0) = \frac{\partial \mathbf{e}(t)}{\partial \mathbf{e}(t_0)}.$$

(Note that it is this same matrix which represents the system dynamics within the matrix A of the differential correction in Eq. (3), there incorporating the state transition between epoch and each of the observation times.) Next, let the matrix G refer to the Jacobian of the transformation between the equinoctial elements, $\mathbf{e}$, and the *uvw* vector space with elements $\mathbf{u}$, as

$$G(t) = \frac{\partial \mathbf{u}(t)}{\partial \mathbf{e}(t)}.$$

If the variation in $\mathbf{u}(t)$ is given by $\Delta\mathbf{u}(t)$, then the linearized representation of this vector, as used in a least squares solution, may be written as

$$\Delta\mathbf{u}(t) = [G(t)\Phi(t,t_0)]\Delta\mathbf{e}(t_0). \tag{4}$$

Now, the covariance in $\mathbf{u}$ space may be formed by combining Eqs. (3) and (4), giving

$$\begin{aligned}\Delta\mathbf{u}(t) &= [G(t)\Phi(t,t_0)]\Delta\mathbf{e}(t_0)\\ &= [G(t)\Phi(t,t_0)]\left(A^{\mathrm{T}}WA\right)^{-1}\left(A^{\mathrm{T}}W\Delta\mathbf{b}\right)\\ &= [G(t)\Phi(t,t_0)]\left(A^{\mathrm{T}}WA\right)^{-1}[G(t)\Phi(t,t_0)]^{\mathrm{T}}[G(t)\Phi(t,t_0)]^{-\mathrm{T}}\left(A^{\mathrm{T}}W\Delta\mathbf{b}\right).\end{aligned}$$

From this result, the covariance in $\mathbf{u}$ space is given by

$$C_u = [G(t)\Phi(t,t_0)]\left(A^{\mathrm{T}}WA\right)^{-1}[G(t)\Phi(t,t_0)]^{\mathrm{T}} = [G(t)\Phi(t,t_0)]C[G(t)\Phi(t,t_0)]^{\mathrm{T}}.$$

The primary reason for the choice of *uvw* vector space is that the position covariance ellipsoid is roughly oriented with principal axes along the *uvw* directions [19]. While the covariance retains its Gaussian character through propagation in orbital element space [20], its physical representation and utility in orbit conjunction assessment are more clearly seen in *uvw* space. Therefore, the covariance propagation is performed using the state transition matrix in equinoctial element space, but the result is produced in *uvw* space.

For purposes of comparison, the principal propagated position covariances were formed by diagonalizing the propagated *uvw* covariance matrix. Fig. 4 shows the behavior of the principal cloud standard deviations in *uvw* vector space throughout the one-day propagation span. In Fig. 4(a), the true standard deviation is seen — note the predominance of the distribution in the transverse (*v*) direction. The ratio of predicted to true standard deviations in each dimension is seen in Fig. 4(b). The predicted standard deviations in each dimension generally remain within an order of magnitude of truth, and the dominant transverse ratio remains near unity. The cloud centroid's position error is shown in Fig. 4(c). These behaviors are consistent with operational orbit determination [19].

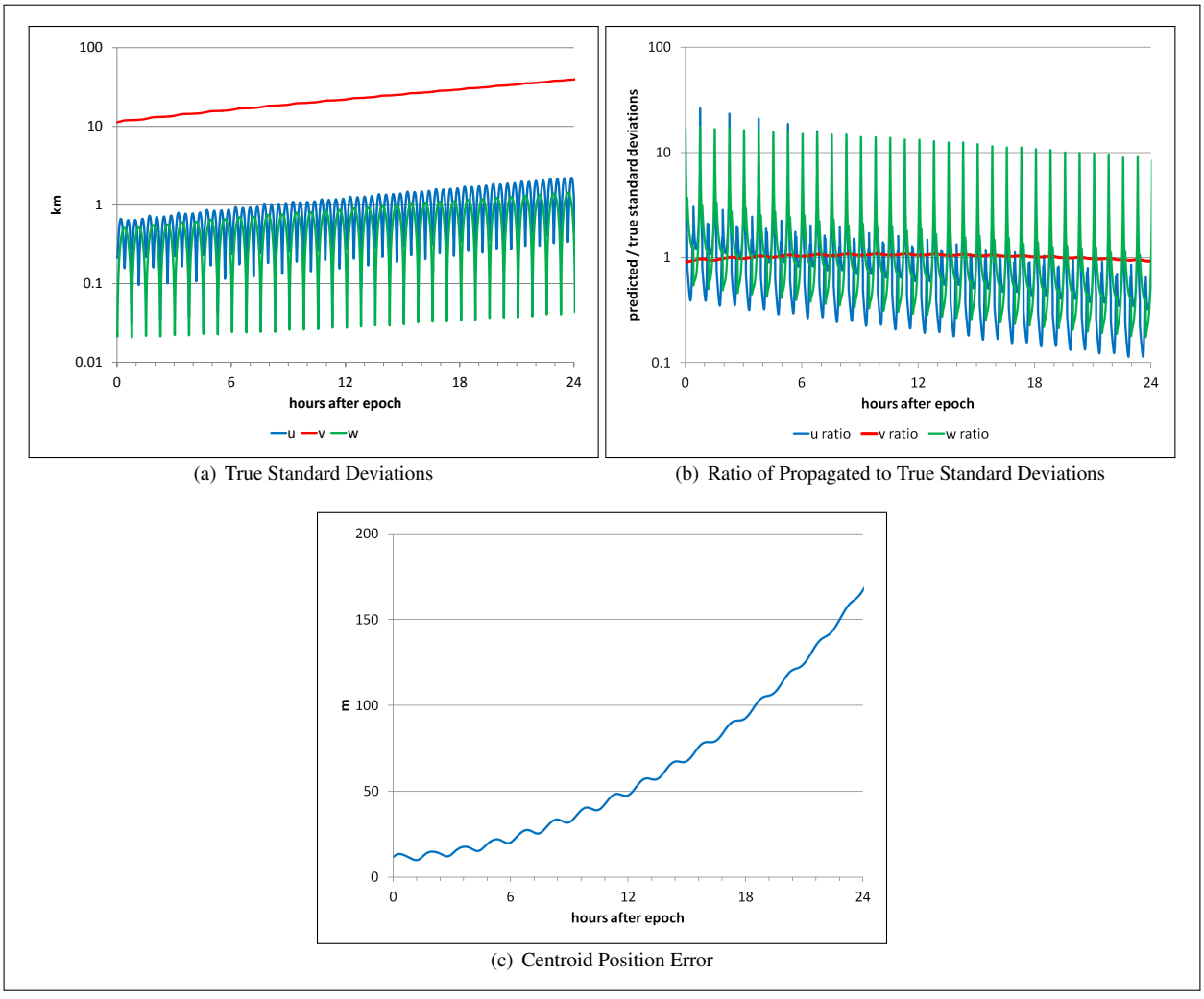

(a) True Standard Deviations

(b) Ratio of Propagated to True Standard Deviations

(c) Centroid Position Error

Fig. 4. Cloud Standard Deviations and Centroid Position Error in *uvw* Space Using Noiseless Observations

This analysis was then repeated, with noise added to the simulated observations used to construct the centroid and variance at each observation time. The noise for each observation was based on the nominal Eglin observation standard deviations for low earth orbits, given in Table 2. The analysis was performed in a Monte Carlo fashion, using 1000 separate random simulations of the observations, with each chip location augmented by a random draw based upon the nominal Eglin standard deviations. In each of the 1000 runs, an orbit determination was performed,

Table 2. Observation Standard Deviations

azimuth	0.017 deg
elevation	0.0197 deg
range	27.705 m

the resulting state and covariance propagated through the subsequent day, and the performance computed. For these orbit determinations, the weights were again determined using the variances of the cloud distributions in observation space. These weights thereby included the contributions of both the sensor observation noise and the actual cloud distribution.

The results of these simulations are shown in Fig. 5. In Fig. 5(a) are the mean ratios of predicted to true standard deviations in *uvw* position space; standard deviations of the ratios are 2-3 orders of magnitude smaller than the mean ratios. Here, the ratios are larger than in the noise-free simulation; however, once again, the dominant transverse distribution ratio (*v* direction) remains close to unity. The cloud centroid's mean position error is shown in Fig. 5(b), along with the position error below which 90% of the 1000 simulations lie. While larger than the case with no noise, the behavior exhibited in Fig. 5 remains close to that for operational orbit determination of a single satellite, rendering it potentially useful for orbital conjunction predictions and probability of collision computations using actual radar observation capabilities.

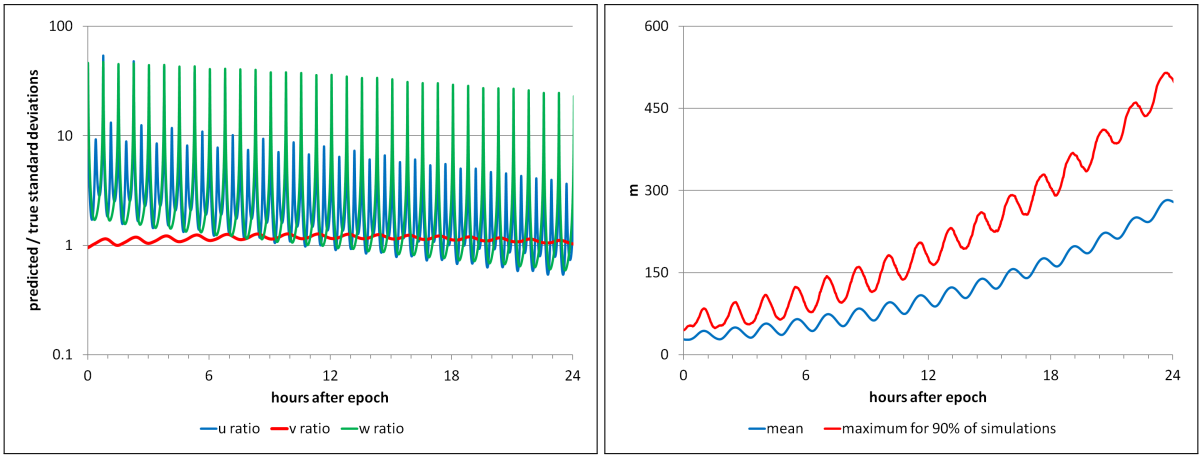

(a) Ratio of Propagated to True Standard Deviations

(b) Centroid Position Error

Fig. 5. Cloud Mean Standard Deviations and Centroid Position Error in *uvw* Space Using Noisy Observations

5. SUMMARY AND CONCLUSION

The large scale deployments of small spacecraft present new challenges to space object cataloging. Two of these challenges are the rapid identification of individual cubesats within a large deployment and the cataloging of a picosat deployment in a manner that is useful for orbital collision assessment.

Cubesat operators require rapid identification of their spacecraft in order to conduct their investigations and experiments during the cubesats' brief orbital lifetimes. With the increasing number and frequency of cubesat deployments, the cubesat community has already begun to investigate and develop methods to speed this identification. Some of these methods involve using beaconing transponders for directional observation collection and location transmission from onboard GPS receivers. The transmission of GPS locations via communication satellite constellations would enable precise and rapid cubesat identification.

Deployments of picosats such as those in the sprite class envisioned by the Kicksat experiment present a distinct cataloging challenge, as current space surveillance capabilities do not permit the reliable tracking of individual chips.

However, space surveillance of a chip cloud may be maintainable through the use of a probabilistic description of the cloud configuration. Such a description can be provided using current operational methods by using the cloud distribution statistics in a batch least squares orbit determination. A simplified analysis has shown that using only a single day's observations from a surveillance radar could permit cataloging of the chip cloud and predicting the subsequent extent of the cloud. Future study of this approach could focus on more realistic simulations of the cloud observations as well as analysis of the method's application to a wide variety of chip carrier orbits and chip deployment scenarios.

6. ACKNOWLEDGEMENT

This work was supported by the Office of the Assistant Secretary of Defense for R&E, via the Data-to-Decisions program, and by the Office of Naval Research.

7. REFERENCES

1. Barrows, S.P., Swinerd, G.G., and Crowther, R., "Review of Debris-Cloud Modeling Techniques," *Journal of Spacecraft and Rockets,* Vol. 33, No. 4, 550–555, 1996.
2. Swinerd, G.G., Barrows, S.P., and Crowther, R., "Short-Term Debris Risk to Large Satellite Constellations," *Journal of Guidance, Control, and Dynamics,* Vol. 22, No. 2, 291–295, 1999.
3. Space-Track, `https://www.space-track.org`, retrieved July 25, 2014.
4. Zarya, `http://www.zarya.info`, retrieved August 3, 2014.
5. National Space Science Data Center, NASA, `http://nssdc.gsfc.nasa.gov`, retrieved July 29, 2014.
6. "Cubesat – General mailing list for CubeSat related information," `http://lists.cubesat.org`, posting June 20, 2014.
7. DeBenedictis, T., Southern Stars Group, private communication, July 31, 2014.
8. Palo, S.E., University of Colorado, private communication, July 23, 2014.
9. Sponable, J., DARPA Tactical Technology Office, private communication, May 6, 2014.
10. Babuscia, A., Corbin, B., Jensen-Clem, R., et al., "CommCube 1 and 2: A CubeSat Series of Missions to Enhance Communication Capabilities for CubeSat," IEEE Aerospace Conference, Big Sky, Montana, 2013.
11. Voss, H.D., Dailey, J.F., Crowley, J.C., et al., "TSAT Globalstar ELaNa-5 Extremely Low-Earth Orbit (ELEO) Satellite," 28th Annual AIAA/USU Conference on Small Satellites, Logan, Utah, 2014, Paper No. SSC14-WK-6.
12. Glennon, E., Parkinson, K., Mumford, P., et al., "A GPS Receiver Designed for Cubesat Operations," Australian Space Science Conference, Canberra, 2011.
13. Barker, W.N., Casali, S.J., and Walker, C.A.H., "Improved Space Surveillance Network Observation Error Modeling and Techniques for Force Model Error Mitigation," AAS/AIAA Astrodynamics Specialist Conference, Girdwood, Alaska, 1999, Paper No. AAS 99-420.
14. Manchester, Z., Peck, M., and Filo, A., "KickSat: A Crowd-Funded Mission to Demonstrate the World's Smallest Spacecraft," 27th Annual AIAA/USU Conference on Small Satellites, Logan, Utah, 2013, Paper No. SSC13-IX-5.
15. Atchison, J.A. and Peck, M.A., "Length Scaling in Spacecraft Dynamics," *Journal of Guidance, Control, and Dynamics,* Vol. 34, No. 1, 231–246, 2011.
16. Manchester, Z.R. and Peck, M.A., "Stochastic Space Exploration with Microscale Spacecraft," AIAA Guidance, Navigation, and Control Conference, Portland, Oregon, 2011, Paper No. AIAA 2011-6648.
17. Neal, H., Coffey, S., and Knowles, S., "Maintaining the Space Object Catalog with Special Perturbations," AAS/AIAA Astrodynamics Specialist Conference, Sun Valley, Idaho, August, 1997, Paper No. 97-687.
18. Arsenault, J.L., Ford, K.C., and Koskela, P.E., "Orbit Determination Using Analytic Partial Derivatives of Perturbed Motion," *AIAA Journal*, Vol. 8, No. 1, 4–12, 1970.
19. Segerman, A.M. and Akins, K.A., "Covariance as a Metric for Catalog Maintenance Error," AAS/AIAA Space Flight Mechanics Meeting, Tampa, 2006, Paper No. AAS 06-233.
20. Junkins, J.L., Akella, M.R., and Alfriend, K.T., "Non-Gaussian Error Propagation in Orbital Mechanics," *Journal of the Astronautical Sciences,* Vol. 44, No. 4, 541-563, 1996.